A comparison of gravimetric geoid models over Western Australia, computed using modified forms of Stokes's integral

W E Featherstone

School of Spatial Sciences, Curtin University of Technology, GPO Box U1987, Perth WA 6845
email: *tfeather@cc.curtin.edu.au*

Abstract

Gravimetric models of the geoid over Western Australia have been constructed using two adapted forms of Stokes's integral; one uses the unmodified Stokes kernel and the other uses a deterministically modified kernel. These solutions use a combination of the complete expansion of the EGM96 global geopotential model with Australian gravity and terrain data. The resulting combined solutions for the geoid are compared with the control given by Global Positioning System (GPS) and Australian Height Datum heights at 63 points over Western Australia. The improved fit of the model that uses a modification to Stokes's kernel indicates that this approach is more appropriate for gravimetric geoid computations over Western Australia.

Introduction

The geoid is the equipotential surface of the Earth's gravity field, which corresponds most closely with mean sea-level (ignoring oceanographic effects) and undulates with respect to an oblate ellipsoidal model of the figure of the Earth. In 1849, GG Stokes published a solution to the geodetic boundary-value problem, which requires a global integration of surface gravity data over the Earth to compute the separation (N) between the geoid and reference ellipsoid (Stokes 1849). However, the incomplete global coverage and availability of accurate gravity measurements has precluded an exact determination of the geoid using Stokes's formula. Instead, an approximate solution is used in practice, where only gravity data in and around the computation area are used. This approach is also attractive because of the increase in computational efficiency that is offered by working with a smaller integration area.

In 1958, MS Molodensky (cited in Molodensky *et al.* 1962) proposed a modification to Stokes's formula to reduce the truncation error that results when gravity data are used over a limited area. However, Molodensky's modification did not receive a great deal of attention at that time because of the contemporaneous availability of low-frequency global gravity field information, derived from the analysis of the orbits of artificial Earth satellites. These global geopotential models are expressed in terms of fully normalised spherical harmonic functions and are now routinely used in conjunction with terrestrial gravity data via a truncated form of Stokes's integral (*e.g.* Vincent & Marsh 1973; Sideris & She 1995). This combined approach reduces the truncation error because its series expansion begins at a higher degree, where the truncation coefficients are smaller in magnitude (assuming that the global geopotential model is an exact fit to the low-degree terrestrial gravity field). Another advantage of this combined solution for the geoid is that it reduces the

impact of the spherical approximation inherent to the derivation of Stokes's integral (*e.g.* Heiskanen & Moritz 1967), the reason being that most of the geoid's power is contained in the low frequencies.

This paper will briefly review the approaches currently used in regional gravimetric geoid computations and presents a compromise approach based on a high-degree global geopotential model and a low-degree modified Stokes kernel (Featherstone *et al.* 1998). An empirical comparison between gravimetric geoid models computed for Western Australia using the unmodified Stokes kernel and the compromise approach will be made with 63 discrete geoid heights. From these comparisons, it will be concluded that the compromise approach is more appropriate for gravimetric geoid computations in Western Australia.

The generalised Stokes scheme

A formal representation of the combination of a global geopotential model with terrestrial gravity data has been proposed by Vaníček & Sjöberg (1991), which they refer to as the generalised Stokes scheme for geoid computation. Importantly, this satisfies a solution to the geodetic boundary-value problem when formulated for a higher than second-degree reference model of the figure of the Earth (Martinec & Vaníček, 1996). In this scheme, the low-frequency geoid undulations generated by a global geopotential model (N_M) are extended into the high frequencies by a global integration of complementary high-frequency, terrestrial gravity anomalies (Δg^M) using

$$N = N_M + \kappa \int_0^{2\pi} \int_0^\pi S^M(\cos\psi)\,\Delta g^M\,\sin\psi\,d\psi\,d\alpha \qquad (1)$$

where $\kappa = R/4\pi\gamma$, R is the spherical Earth radius, γ is normal gravity evaluated on the surface of the geocentric reference ellipsoid as required by Bruns's formula (*e.g.* Heiskanen & Moritz 1967), ψ and α are the coordinates of spherical distance and azimuth angle about the

computation point, respectively, and $S^M(\cos\psi)$ is the spheroidal form of Stokes's integration kernel, which is implicit to the generalised scheme and has the series expansion

$$S^M(\cos\psi) = \sum_{n=M+1}^{\infty} \frac{2n+1}{n-1} P_n(\cos\psi) \qquad (2)$$

where $P_n(\cos\psi)$ is the nth degree Legendre polynomial.

In Eq (1), the low-frequency component of the geoid (N_M) is computed from the fully normalised spherical harmonic coefficients that define the global geopotential model according to

$$N_M = \frac{GM_e}{r\gamma} \sum_{n=2}^{M} \left(\frac{a}{r}\right)^n \sum_{m=0}^{n} (\delta\overline{C}_{nm}\cos m\lambda + \overline{S}_{nm}\sin m\lambda)\overline{P}_n^m(\cos\theta)$$

$$(3)$$

The corresponding high-frequency gravity anomalies (Δg^M) are evaluated by subtracting the same spherical harmonic degrees of the same global geopotential model from the terrestrial gravity anomalies (Δg) according to

$$\Delta g^M = \Delta g - \frac{GM_e}{r^2} \sum_{n=2}^{M} \left(\frac{a}{r}\right)^n (n-1) \sum_{m=0}^{n} (\delta\overline{C}_{nm}\cos m\lambda + \overline{S}_{nm}\sin m\lambda)\overline{P}_n^m(\cos\theta)$$

$$(4)$$

In Eqs (3) and (4), GM_e is the product of the Newtonian gravitational constant and mass of the solid Earth, oceans and atmosphere, a is the equatorial radius of the reference ellipsoid, (r, θ, λ) are the geocentric spherical polar coordinates of each computation point, $\delta\overline{C}_{nm}$ and $\overline{S}_{nm}$ are the fully normalised geopotential coefficients of degree n and order m, which have been reduced by the even zonal harmonics of the reference ellipsoid, and $\overline{P}_{nm}(\cos\theta)$ are the fully normalised associated Legendre functions. It is assumed that the reference ellipsoid is geocentric and has the same mass, potential and rotation rate as the geoid, such that the zero and first degree harmonics are inadmissible (*e.g.* Heiskanen & Moritz 1967).

The degree (M) of reference spheroid chosen for the generalised Stokes scheme can be driven by the maximum degree of global geopotential model available, which is usually M_{max} = 360. However, there are more important considerations than simply taking the maximum degree of expansion available (*e.g.* Featherstone 1992). Firstly, the M_{max} = 360 models are already combined solutions for the geoid because they are constructed from both satellite-derived and terrestrial gravity data. Therefore, the same terrestrial gravity data are usually used twice in Eq (1), which gives rise to unknown correlations between these data that are rarely accounted for or even acknowledged by some authors. Another consideration is the leakage of low-frequency errors from the terrestrial gravity anomalies into the combined solution for the geoid, which can be filtered by the spheroidal kernel due to the orthogonality of spherical harmonic functions over the sphere (*e.g.* Vaníček & Featherstone 1998). This is considered to be a desirable scenario because the low-frequency geopotential coefficients are currently the best source of this information, whereas terrestrial gravity data are subject to low-frequency errors. Therefore, choosing the degree of spheroid at, say, M = 20 in Eq (1), which is the limit of the reliable resolution of the satellite-derived

geopotential coefficients, both avoids the correlations and reduces the leakage of terrestrial gravity anomaly errors.

Reduction of the Approximation Error

The generalised Stokes scheme

The generalised Stokes scheme (Eq 1) remains subject to a truncation error when high-frequency terrestrial gravity anomalies are used over a limited area. Accordingly, there is an adjustment of Eq (1) that involves limiting the integration domain to a spherical cap of radius ψ_0 ($0 - \psi_0 - \pi$) about each geoid computation point, which yields the approximation

$$N \simeq \hat{N}_1 = N_M + \kappa \int_0^{2\pi} \int_0^{\psi_0} S^M(\cos\psi)\,\Delta g^M\,\sin\psi\,d\psi\,d\alpha$$

$$(5)$$

with a corresponding truncation error of

$$\delta N_1 = \kappa \int_0^{2\pi} \int_{\psi_0}^{\pi} S^M(\cos\psi)\,\Delta g^M\,\sin\psi\,d\psi\,d\alpha \qquad (6)$$

such that $N = \hat{N}_1 + \delta N_1$. This truncation error can be expressed as a series expansion by

$$\delta N_1 = 2\pi\kappa \sum_{n=M+1}^{\infty} Q_n^M(\psi_o)\,\Delta g_n \qquad (7)$$

where the spheroidal truncation coefficients

$$Q_n^M(\psi_o) = \int_{\psi_o}^{\pi} S^M(\cos\psi)\,P_n(\cos\psi)\,\sin\psi\,d\psi \qquad (8)$$

can be evaluated using the algorithms of Paul (1973). The nth degree surface spherical harmonic of the gravity anomaly can be evaluated for each n up to the maximum degree (M_{max}) of the geopotential model using

$$\Delta g_n = \frac{GM}{r^2} \left(\frac{a}{r}\right)^n (n-1) \sum_{m=0}^{n} (\delta\overline{C}_{nm}\cos m\lambda + \overline{S}_{nm}\sin m\lambda)\overline{P}_n^m(\cos\theta)$$

$$(9)$$

As such, the truncation error in Eq (7) reduces to

$$\delta N_1 = 2\pi\kappa \sum_{n=M_{max}+1}^{\infty} Q_n^M(\psi_o)\,\Delta g_n \qquad (10)$$

However, if $\Delta g^M \bullet 0$ (2 - n - M), which is true if the global geopotential model is not an exact fit to the low-frequency terrestrial gravity anomalies, Eq (10) no longer holds and there is a leakage of any low-frequency gravity errors into the geoid solution when the integration is performed over a limited area (Vaníček & Featherstone 1998). This is a direct consequence of the approximation of the generalised Stokes integral, which introduces the non-zero truncation coefficients in the region 2 - n - M because the orthogonality of spherical harmonics over the sphere breaks down under the approximation in Eq (5). Since Δg_n only depend on the physical properties of the Earth, it becomes necessary to seek a modification to the integration kernel that reduces the magnitude of the truncation coefficients and hence the truncation error. Ideally, this modification should reduce the truncation error as well as adapting the kernel to behave as a (partial) high-pass filter and thus reduce the leakage of any low-frequency terrestrial gravity data errors into the geoid (Vaníček & Featherstone 1998).

The remove-compute-restore scheme

The remove-compute-restore technique (*e.g.* Torge 1991) has almost become a standard approach in regional combined solutions for the geoid. However, most users of this approach make no attempt to modify the integration kernel and thus (further) reduce the truncation error or adapt its filtering properties. Instead, this scheme uses the unmodified kernel as originally introduced by Stokes (*e.g.* Sideris & She 1995; Smith & Milbert 1999). The remove-compute-restore approach also generally uses the maximum available degree of the global geopotential model (M_{max}), which gives rise to the approximated data combination

$$N \simeq \hat{N}_2 = N_{M_{max}} + \kappa \int_0^{2\pi} \int_0^{\psi_0} S(\cos\psi)\,\Delta g^{M_{max}}\,\sin\psi\,d\psi\,d\alpha$$

(11)

where the terms N_{Mmax} and Δg^{Mmax} are computed from the maximum available degree and order of a global geopotential model (Eqs. 3 and 4), and the unmodified Stokes kernel is given by

$$S(\cos\psi) = \sum_{n=2}^{\infty} \frac{2n+1}{n-1} P_n(\cos\psi)$$

(12)

In this combined solution for the geoid, the truncation error for degrees greater than M_{max} has to be neglected because it cannot be computed since the complete expansion of the global geopotential model has already been used. This also makes it subject to the correlation of errors between the global geopotential model and terrestrial gravity data used in the regional geoid solution. Moreover, no other attempt has been made to reduce the truncation error or adapt the filtering properties of the integration kernel. Admittedly, the truncation error will reduced a great deal if the global geopotential model is a good fit to the terrestrial gravity anomalies in the area of interest (*i.e.* if $\Delta g^M = 0$ in the region $2 - n - M_{max}$). However, the penalty of taking this approach is that any errors in the terrestrial gravity anomalies to propagate unattenuated into the combined solution for the geoid (Vaníček & Featherstone 1998). It must also be acknowledged that, despite these restrictions, the remove-compute-restore technique has delivered quite reasonable results (*e.g.* Sideris & She 1995; Smith & Milbert 1999). However, the question of whether a modified integration kernel in the generalised Stokes scheme will deliver even better results remains, and thus forms the primary aim of this investigation.

Integration kernel modifications

As argued above, it remains preferable to apply a modification to the approximated form of the generalised Stokes's integral (Eq 5) and the remove-compute-restore approach (Eq 11) so as to further reduce the associated truncation error. Since Molodensky's pioneering work, several other authors have proposed modifications to Stokes's (1849) integral. These have been based on different criteria and can be broadly classified as deterministic modifications (*e.g.* Molodensky *et al.* 1962; Wong & Gore 1969; Meissl 1971; Heck & Grüninger 1987; Vaníček & Kleusberg 1987; Vaníček & Sjöberg 1991; Featherstone *et al.* 1998) and stochastic modifications (*e.g.* Wenzel 1982; Sjöberg 1991; Vaníček & Sjöberg 1991). The stochastic modifications, whilst offering an optimal

combination of the two data types together with a minimisation of the truncation error (in a least-squares sense), require reliable variance estimates of the data. However, the error characteristics of the terrestrial gravity data over Western Australia and over most other parts of the world are currently unknown, which renders the stochastic modifications of limited practical use. Therefore, the deterministic kernel modifications will have to be relied upon in the interim.

The deterministic kernel modifications can be further divided into two broad categories; modifications that reduce the upper bound of the truncation error according to some prescribed norm, and modifications that improve the rate of convergence of the series expansion of the truncation error. The modification proposed by Featherstone *et al.* (1998) uses a combination of these, where the rate of convergence of the series expansion of an already-reduced truncation error by the L_2 norm (Vaníček & Kleusberg 1987) is accelerated from $\tilde{O}(n^{-1})$ to $O(n^{-2})$ through the approach proposed by Meissl (1971). This can be achieved either by setting the kernel to zero at the truncation radius through subtraction, or by choosing the truncation radius such that it coincides with a zero point of the kernel.

The Featherstone *et al.* (1998) modification is given by

$$S_L^M(\cos\psi) = S^M(\cos\psi) - S^M(\cos\psi_0) - \sum_{k=2}^{L} \frac{2k-1}{2} t_k(\psi_0)\left[P_k(\cos\psi) - P_k(\cos\psi_0)\right]$$

(13)

where the $t_k(\psi_0)$ modification coefficients are computed from the solution of the following set of L-1 linear equations, once the truncation radius (ψ_0) has been chosen

$$\sum_{k=2}^{L} \frac{2k+1}{2} t_k(\psi_0)\,e_{nk}(\psi_0) = Q_n^M(\psi_0)$$

(14)

where the coefficients $Q^M_n(\psi_0)$ are given by Eq (8), and

$$e_{nk}(\psi_0) = \int_{\psi_0}^{\pi} P_n(\cos\psi) P_k(\cos\psi) \sin\psi\,d\psi$$

(15)

which can be evaluated using the recursive algorithms of Paul (1973). The degree of this kernel modification (L) can be chosen to be greater than, equal to or less than the degree of the reference spheroid (M) embedded in the generalised Stokes formula (Eq 1). If $L > M$, additional terms arise due to this disparate combination and should be computed or their omission acknowledged.

A compromise of the combined solution

The combined solution for the geoid considered in this study attempts to reach a compromise of the above two schemes, based on considerations of the data availability, their expected reliability, and a reduction of the truncation error through the above deterministic modification of the generalised Stokes kernel. This compromise approach was used to compute the recent Australian gravimetric geoid model, AUSGeoid98 (Johnston & Featherstone 1998). Mathematically, this is formalised as

$$N \simeq \hat{N}_3 = N_{M_{max}} + \kappa \int_0^{2\pi} \int_0^{\psi_0} S_L^M(\cos\psi)\,\Delta g^{M_{max}}\,\sin\psi\,d\psi\,d\alpha$$

(16)

where all terms are as defined earlier. Equation (16) utilises the maximum available expansion (M_{max}) of the global geopotential model in conjunction with a low-degree (L) of deterministic kernel modification. This approach aims at reducing the truncation error so that it can be safely ignored, whilst relying more on the low-degree satellite solution by filtering a proportion of the low-frequency errors from the terrestrial gravity data (*cf.* Vaníček & Featherstone 1998). However, this choice is also driven by some practical considerations. Empirical studies by Featherstone (1992) indicate that the modified kernels become numerically unstable for large L and small ψ_0, which enforces a low degree of kernel modification when a small integration radius is used. For simplicity, the degree of kernel modification is chosen equal to the degree of spheroid used in the generalised scheme (*i.e.* $L = M = 20$). The integration radius was chosen to be $\psi_0=1°$, since this value was empirically selected for AUSGeoid98 (Johnston & Featherstone 1998).

It is argued that this compromise approach offers a geoid solution that is superior to the application of the remove-compute-restore technique with an unmodified kernel because of its further reduction of the truncation error and adaption of the filtering properties of the kernel. However, it is also important to acknowledge the deficiencies of this attempted compromise, which are the use of the high-frequencies in the global geopotential model (which can contain 80% noise; *e.g.* Lemoine *et al.* 1998) and the correlations between the terrestrial gravity data in the region $20 < n - M_{max}$. Therefore, empirical tests are used in Western Australia to determine whether the use of a deterministically modified integration kernel is more appropriate than using the unmodified kernel.

Empirical tests in Western Australia

The tests that follow compare four combined solutions for the geoid, computed using differing parameters in Eqs (11) and (16), with discrete geoid heights at 63 points across Western Australia. These control data are derived from Global Positioning System (GPS) measurements at Australian Height Datum (AHD) benchmarks. The difference between a GPS-derived ellipsoidal height and geodetically levelled height with respect to mean sea level gives a discrete estimate of the separation between the geoid and reference ellipsoid. Assuming that there are no errors in these control data, the gravimetric geoid solution that delivers the best fit can be considered to be the most suitable for Western Australia.

Data and its processing

The EGM96 global geopotential model (Lemoine *et al.* 1998), complete to $M_{max} = 360$, was used in this study. EGM96 is one of the most recent global geopotential models and was produced by the US National Imagery and Mapping Authority (NIMA), formerly the Defense Mapping Agency (DMA), and the US National Aeronautical and Space Administration's (NASA) Goddard Space Flight Center (GSFC). Kirby *et al.* (1998) compared EGM96 with Australian gravity data (described below) and discrete geoid heights provided by co-located GPS and AHD data (also described below). This showed that EGM96 provides a slightly better

(though statistically not significant) representation of the Australian gravity field than its predecessors.

The Australian Geological Survey Organisation's (AGSO) 1996 national gravity data release, being the most recent available to the author, has been used in the computations. As most of the AGSO gravity data were collected and reduced predominantly for geophysical exploration purposes, they are not necessarily suited to the requirements of gravimetric geoid computation. As such, they have been validated according to the procedures in Featherstone *et al.* (1997) and the gravity anomalies computed using the more stringent geodetic approaches (*e.g.* Featherstone & Dentith 1997). Deficiencies were also found in the mean free-air gravity anomalies computed on land, due to the gravity data collection strategies used by AGSO. The land gravity observations were typically made along roads and tracks in areas of rugged terrain, which usually follow valleys or areas of least height variation. A similar, though opposite, effect occurs in central Australia where most observations were performed using helicopter transport. These observations were often located on raised ground where convenient landing spots were identified. Specifically, the computed mean gravity anomaly does not truly represent the actual mean gravity anomaly of an area. As such, the computed gravimetric geoid is biased by these gravity observation techniques. To numerically counter this biasing effect, a digital elevation model (described below), which gives a better representation of the mean terrain height than the gravity observation elevations, was used to reconstruct more representative mean gravity anomalies (Featherstone & Kirby 2000).

Satellite-altimeter-derived marine gravity anomalies were used offshore Australia to supplement AGSO's marine gravity data coverage. These gravity anomalies were computed from a combination of satellite-borne radar altimeter missions and supplied on a 2' by 2' geographical grid (Sandwell & Smith 1997). These data significantly improve the gravity data coverage offshore Australia and, as such, were expected to give an improved geoid solution in marine areas and on land areas close to the coast. However, errors thought to reside in the low-frequency altimeter-derived gravity anomalies adversely affect the gravimetric geoid near the coast, which was indicated by comparisons of the geoid solution with GPS and AHD data on land near the coast. The low-frequency errors in the satellite altimeter data are probably due to a combination of poorly-modelled near-shore sea-surface topography, tides and backscatter of altimeter returns from the land. Another explanation for this observed deficiency comes from the conversion of sea surface heights, which are the direct measurements taken by the altimeter, to gravity anomalies, then converting these gravity anomalies to geoid heights. At present, it is unknown how the errors, such as poorly-modelled sea-surface topography, propagate through these processes. Therefore, as an interim and practical solution, least squares collocation (*e.g.* Moritz 1980a) was used to 'drape' the altimeter gravity anomalies onto the AGSO marine gravity anomalies (Kirby & Forsberg 1998). This approach then improved the geoid solution on land near the coast, when compared with GPS and AHD data, over that achieved using only the AGSO marine gravity

data or simple averaging of the AGSO marine gravity data and the satellite-altimeter data.

Gravimetric terrain corrections, based on the national 9" by 9" digital elevation model (Carrol & Morse 1996), were evaluated using Moritz's (1968) formula via the fast Fourier transform or FFT (Kirby & Featherstone 1999). The FFT offers the only practical way to compute detailed terrain corrections on a continental scale, since prism integration at this scale could take several months to evaluate. It was found by Kirby & Featherstone (1999) that the terrain correction computations had to be performed using a 27" by 27" grid to avoid the instability in Moritz's terrain correction algorithm that occurs when using high-resolution digital terrain models close to the computation point (*cf.* Martinec *et al.* 1996). Associated with the gravimetric terrain correction are the primary and secondary indirect effects (*e.g.* Wichiencharoen 1982). The primary indirect effect accounts for the change in potential caused by the free-air gravity reduction and gravimetric terrain correction. The primary indirect effect was computed using the FFT on a 27" grid, which avoids the kernel instability and, moreover, is consistent with the terrain correction computations. The secondary indirect effect on gravity was computed by applying the free-air reduction over the geoid-compensated-geoid separation computed via the primary indirect effect. This resulted in an additional gravity term that was added to the gravity anomalies prior to geoid computation.

A grid of residual gravity anomalies was computed from the AGSO gravity observations using the continuous curvature spline in tension algorithm (Smith & Wessel 1990; Wessel & Smith 1995). The term residual gravity anomalies is used to describe the terrain-corrected free-air gravity anomalies that have been reduced by the gravity anomalies implied by the complete M_{max} = 360 expansion of EGM96 (Eq 4). A regular grid of residual gravity anomalies is required for the residual geoid computations via the one-dimensional FFT technique. It is acknowledged that other gravity gridding techniques exist, such as least squares collocation (Moritz 1980a), but the continuous curvature spline in tension algorithm was readily available (Wessel & Smith 1995) and gives almost identical results in a considerably shorter computation time (Zhang 1997). For this study, a 2' by 2' grid of gravity anomalies was generated over the region by -11° - ϕ - -37° and 110° - λ - 131°, which covers the state of Western Australia. Table 1 summarises the statistical properties of the gravity anomalies and the residual gravity anomalies. The GRS80 reference ellipsoid (Moritz 1980b) has been used in all computations. Grey-scale images of the EGM96-implied gravity anomalies and residual gravity anomalies are shown in Figs 1 and 2, respectively.

The statistical fit of the gravity anomalies implied by the EGM96 global geopotential model to the gravity field of Western Australia is poorer than that experienced in other parts of the world (*cf.* Forsberg & Featherstone 1998). This is probably due to the larger uncertainty in the terrestrial gravity anomalies, which is caused principally by errors in the gravity station elevations (*e.g.* Featherstone *et al.* 1997). However, since a large proportion of these data has been used in the construction of the EGM96 global geopotential model, a more likely explanation is an inaccuracy in the mean gravity anomalies used
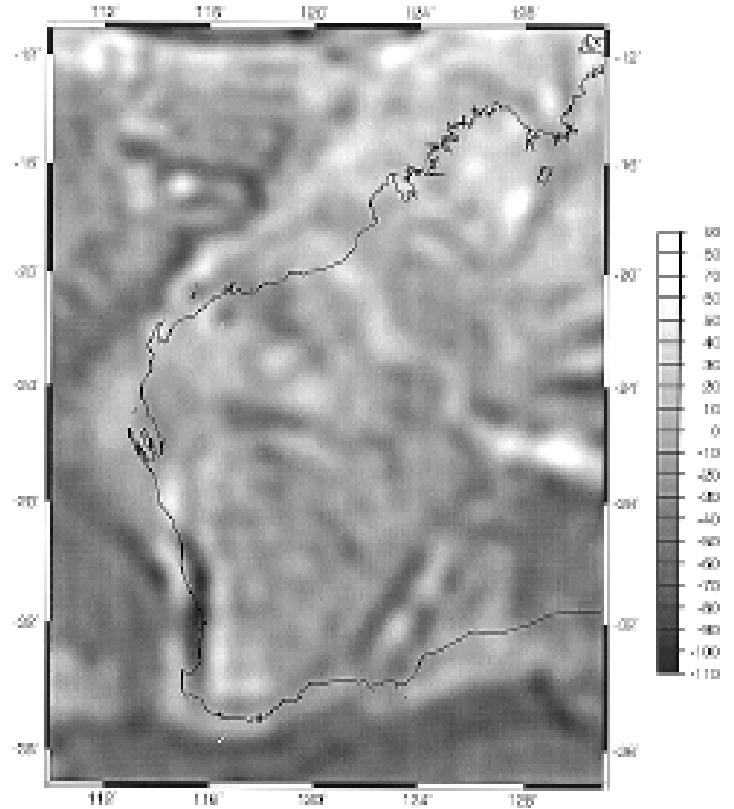

Figure 1. The M_{max} = 360 EGM96-implied gravity anomalies over Western Australia (units in mGal; Mercator's projection from the GRS80 ellipsoid).
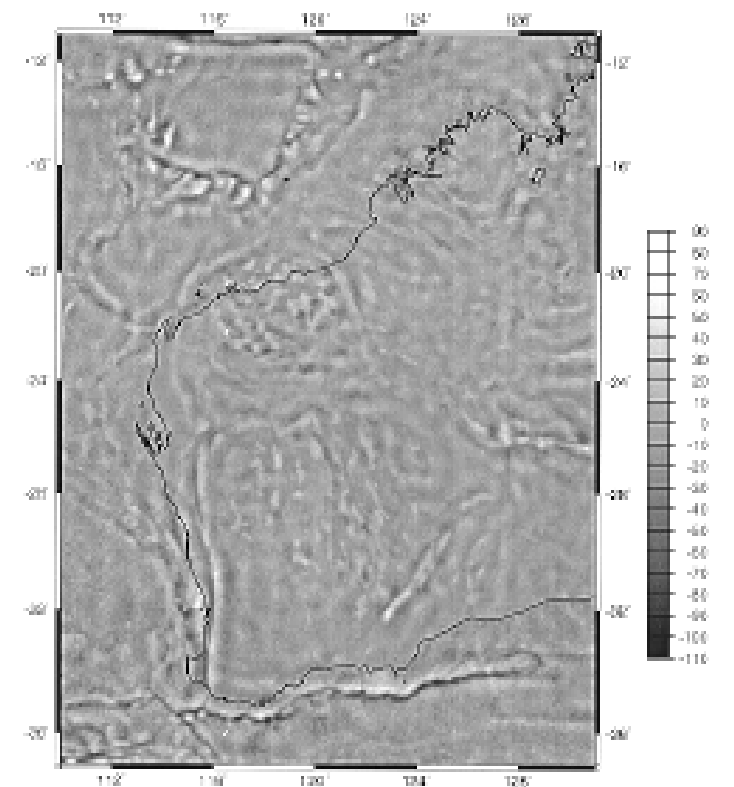

Figure 2. The residual gravity anomalies over Western Australia (units in mGal; Mercator's projection from the GRS80 ellipsoid).

Table 1

Minimum, maximum, mean, standard deviation (SD) and root mean square (RMS) for the gravity anomalies over Western Australia (units in mGal).

gravity anomalies	Minimum	Maximum	Mean	SD	RMS
terrain-corrected free-air	131.085	-147.678	-8.762	± 29.110	± 30.400
residual	91.554	-101.236	0.009	± 10.968	± 10.968

for this model. Lemoine *et al.* (1998) describe the construction of the JGP95E 5' by 5' digital elevation model, where the Australian 5' by 5' digital elevation model was used west of $\lambda = 140°$ and a National Imagery and Mapping Agency (NIMA) digital elevation model was used east of $\lambda = 140°$. The Australian 5' by 5' digital elevation model used by NIMA was probably that constructed at the Australian National University from the elevations associated with the gravity station elevations. Featherstone & Kirby (2000) show that this digital elevation model is biased because the gravity observations do not accurately represent the topographic morphology (see earlier discussion). Therefore, more reliance should be placed on the terrestrial gravity anomalies described earlier, hence the use of a low-degree kernel modification.

Geoid computation by the 1D-FFT technique

In the mid 1980s, the fast Fourier transform (FFT) technique began to find wide-spread use in gravimetric geoid computation, because of its efficient evaluation of convolution integrals when compared to quadrature-based numerical integration. For many years, the planar, two-dimensional FFT was used (*e.g.* Schwarz *et al.* 1990). Strang van Hees (1990) then introduced the spherical, two-dimensional FFT. However, both of these FFT approaches are subject to approximation errors, the most notable of which is the simplification of Stokes's kernel. Forsberg & Sideris (1993) therefore proposed the spherical, multi-band FFT, which reduces the impact of the simplified kernel. Haagmans *et al.* (1993) then refined this approach to give the spherical, one-dimensional FFT, which requires no simplification of Stokes's kernel. For this reason, the 1D-FFT has been used in this investigation so that the exact kernels in Eqs (12) and (13) can be used efficiently and without the need for any simplification.

Another consideration is that remove-compute-restore determinations of the geoid using the 1D-FFT often convolve the whole rectangular grid of gravity anomalies over a region with the spherical Stokes kernel (*e.g.* Sideris & She 1995; Smith & Milbert 1999). On the other hand, quadrature-based geoid determinations only use gravity anomalies over a spherical integration radius about each computation point. Therefore, each approach results in a different truncation error due to the neglect of the residual gravity anomalies in the (different shaped) remote zones outside each integration domain. Both of these implementations are tested in this study, where in Eq (11) the spherical integration radius is set to $\psi_0 = \pi$ so as to use the whole gravity data rectangle, and a limited spherical cap is used to mimic quadrature-based numerical integration.

In order to make the 1D-FFT approach closely mimic quadrature-based numerical integration over a spherical cap, the integration kernel is set to zero outside the truncation radius ($\psi_0 = 1°$) before transformation to the frequency domain. A further adaptation of this technique has been added to allow the 1D-FFT-based evaluation of Eq (16), where the modified kernel (Eq 13) was implemented by evaluating it before transformation to the frequency domain (Featherstone & Sideris 1998). Comparisons with quadrature-based numerical integration software that uses spherical caps and deterministically modified integration kernels (Featherstone, 1992) were used to verify these adaptations of the 1D-FFT.

In what follows, the gravimetric geoid heights from each approach have been evaluated using the 1D-FFT for

(i) the remove-compute-restore technique with an unmodified kernel and residual gravity anomalies over whole data area $\psi_0 = \pi$,

(ii) the remove-compute-restore technique with an unmodified Stokes's kernel and residual gravity anomalies over a limited spherical cap ($\psi_0 = 1°$), and

(iii) the compromise approach in Eq (16) with a deterministically modified integration kernel and residual gravity anomalies over a limited spherical cap ($\psi_0 = 1°$).

In the latter case, the degree of spheroid associated with the generalised Stokes scheme is $M = 20$ and the degree of deterministic kernel modification is the same. Of course, a large number of permutations of these parameters is possible by varying the degree of global geopotential model (*M*), integration radius (ψ_0), degree of kernel modification (*L*), and even the type of kernel modification (see section Integration Kernel Modifications, above). However, only the above three cases are studied for Western Australia because the remove-compute-restore technique is used in many other parts of the world (*e.g.* Sideris & She 1995; Smith and Milbert 1999), and the $L = M = 20$ modification for a cap radius of $\psi_0 = 1°$ was used for AUSGeoid98 (Johnston & Featherstone 1998).

All geoid computations were conducted on a 2' by 2' grid over an area bound by -12° - ϕ - -36° and 112° - λ - 129°, which eliminates the edge effect associated with the one-degree integration radius (with the exception of the integration over the whole data area). It should be pointed out that this edge effect affects the whole computation area when the cap-radius is unlimited. Nevertheless, the geoid comparisons are conducted over the same area for the sake of consistency.

Comparison of Geoid Results with GPS at AHD Benchmarks

As is customary in almost all validations of gravimetric geoid models on land, the geoid results from this study were compared with Global Positioning

System (GPS) and geodetic levelling data to determine if any improvements are made when utilising a spherical integration cap and deterministically modified kernel. However, it must be pointed out this type of comparison is inevitably biased because the geodetic levelling data used in this investigation are based on the Australian Height Datum (AHD). The AHD is a normal orthometric height system based on estimates of mean sea level from 30 tide gauges around Australia (Roelse *et al.* 1971). As such, it does not give an exact representation of the equipotential geoid (*e.g.* Featherstone 1998). Nevertheless, GPS and geodetic levelling data currently provide the only (partially) independent means with which to verify a gravimetric geoid model on land. Given that the primary geodetic application of a gravimetric geoid model is to transform GPS-derived ellipsoidal heights to the AHD, this type of analysis is also useful to ascertain the gravimetric geoid models' performance for this application.

For each of the three cases investigated, the gravimetric geoid solution was bi-cubically interpolated from the 2' by 2' grid and statistically compared with 63 discrete geoid heights. These were derived geometrically from the most precise GPS networks available in Western Australia (Morgan *et al.* 1996; Stewart *et al.* 1997) at points that are co-located with geodetically levelled heights of third-order, or better, on the AHD. Table 2 shows a statistical summary of the differences between the 63 control geoid heights and the results from the $M_{max}=360$ expansion of EGM96 alone (Eq 3), the 1D-FFT implementations of Eq (11) with $\psi_0 = \pi$ and $\psi_0 = 1°$, and Eq (16) with $\psi_0 = 1°$. The mean and root mean square (RMS) differences in Table 2 should not be relied upon to choose the most accurate geoid solution because any gravimetric determination of the geoid is deficient in scale (*i.e.* only the gravimetric geoid's precision can be estimated). This scale deficiency due to the imperfect knowledge of the mass of the Earth [*cf* the text immediately after Eqs (3) and (4)]. Accordingly, only the standard deviations of the fit of each gravimetric geoid model to the control data should be used to assess the performance in terms of precision of each model; the mean and RMS values are only included for the sake of completeness.

The difference between the fit of each geoid model in Table 2 is not always significant in a statistical sense, when considering that the random error budget of the GPS data is ~0.05 m (Morgan *et al.* 1996; Stewart *et al.* 1997) and distortions of the AHD from the geoid are of the order of 1 m (Roelse *et al.* 1971; Featherstone & Stewart 1998; Featherstone 1998). Despite these caveats,

some useful inferences can be made from these results as follows.

Firstly, the use of the whole gravity data area in the combined solution for the geoid (Eq 11 with $\psi_0 = \pi$) gives a result that is worse than using the EGM96 global geopotential model alone (Table 2). Whilst the use of the whole data area appears to be appropriate in other parts of the world (*e.g.* Sideris & She 1995; Smith & Milbert 1999), a considerably worse result is achieved in Australia when using this approach (Table 2; Forsberg & Featherstone 1998; Johnston & Featherstone 1998). This is a slightly unexpected result, since including more data in the geoid solution should yield a better result. This is either due to noise in the Australian gravity anomalies, which been estimated to be approximately ± 2 mGal (Featherstone *et al.* 1997), or the theoretical basis of this approach is unsuitable for Australia.

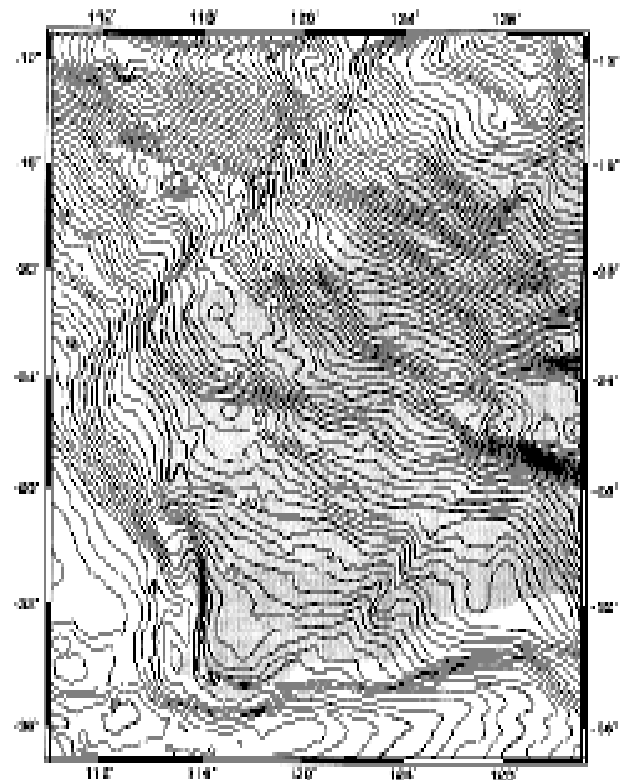Next, from Table 2 there is an improvement over the results of using only the EGM96 global geopotential

Figure 3. The gravimetric geoid over Western Australia, computed using Eq (16) with $\psi_0 = 1°$ and $S_{20}^{20}(\cos \psi)$; units in metres; Mercator's projection from the GRS80 ellipsoid.

Table 2

Minimum, maximum, mean, standard deviation (SD) and root mean square (RMS) for the absolute between the 63 control GPS-AHD heights and the gravimetric geoid heights computed from EGM96 only, Eq (11) with $\psi_0 = \pi$ and $\psi_0 = 1°$ and Eq (16) with $\psi_0 = 1°$ (units in metres).

	Minimum	Maximum	Mean	SD	RMS
$M_{max} = 360$ expansion of EGM96 (Eq 3)	0.889	-0.328	0.148	± 0.274	± 0.311
Eq (11) with $\psi_0 = p$ and $S(\cos \psi)$	0.751	-0.776	-0.092	± 0.362	± 0.374
Eq (11) with $\psi_0 = 1°$ and $S(\cos \psi)$	0.625	-0.664	0.118	± 0.249	± 0.276
Eq (11) with $\psi_0 = 1°$ and $S_{20}^{20}(\cos \psi)$	0.761	-0.308	0.140	± 0.223	± 0.263

represent an equipotential surface of the Earth's gravity field (Featherstone 1998). However, the possibility of systematic errors in the gravimetric geoid cannot be ruled out as an explanation for these discrepancies.

Conclusion

From these gravimetric geoid results over Western Australia, it is clear that 1D-FFT geoid computations should use a spherical cap of limited extent instead of the whole gravity data grid. Small (though not statistically significant when considering the errors in the GPS and AHD data) improvements are also observed when a deterministically modified integration kernel is used over a spherical cap in the compromise approach to gravimetric geoid determination (Eq 16). This improvement is probably because the kernel modification reduces the truncation error so that its neglect has less impact on the solution and adapts the filtering properties of the kernel thereby reducing the effect of low-frequency terrestrial gravity anomaly errors. Therefore, it is recommended that limited integration caps and modified Stokes's kernels are used in spectral geoid determinations

model offered by the use of a limited integration radius in Eq (11). Importantly, there is a further improvement offered by using the deterministically modified integration kernel in Eq (16) for the same integration radius. Though inconclusive due to the perceived uncertainties in the control data, these results do indicate that the use of deterministically modified integration kernel is a preferable approach for geoid computations in Western Australia. This is bearing in mind that the principal application of the gravimetric geoid in Australia is to transform GPS-derived ellipsoidal heights to the AHD. Fig 3 shows a contour map of the gravimetric geoid model of Western Australia that has been computed using Eq (16) with $y_0 = 1°$ and $L = M = 20$.

Finally, it is informative to view the geographical distribution of the discrepancies between the 63 GPS-AHD discrete geoid heights and the gravimetric geoid computed from the modified Stokes integral (Fig 4). There are systematic differences between the gravimetric geoid and the control data, where these features (highs, lows and slopes) are defined by more than one control point. Given the relatively small error budget of the GPS data (^{a} 0.05 m), it becomes difficult to ascertain whether these systematic differences are due to distortions in the AHD, the gravimetric geoid, or both. It is currently impossible to isolate the exact source, but following the arguments in Featherstone & Stewart (1998), it is more likely that these errors are due to distortions in the AHD. These are introduced because the AHD is constrained to mean sea level observed over two years at 30 tide gauges around Australia (Roelse et al 1971) and thus does not necessarily

Featherstone W E, Kearsley A H W & Gilliland J R 1997 Data preparations for a new Australian gravimetric geoid. The Australian Surveyor 42:33-44.

Forsberg R & Sideris M G 1993 Geoid computations by the multi-band spherical FFT approach. Bulletin G'eod'esique 18:82-90.

Forsberg R & Featherstone W E 1998 Geoids and cap sizes. In: Geodesy on the Move: Gravity, Geoids, Geodynamics, and Antarctica (eds R Forsberg, M Feissl & R Dietrich). Springer, Berlin, 194-200.

Heck B & Grüninger W 1987 Modification of Stokes's Integral Formula by Combining Two Classical Approaches. IUGG General Assembly, Vancouver, Canada.

Haagmans R R, de Min E & van Gelderen M 1993 Fast evaluation of convolution integrals on the sphere using 1D-FFT, and a comparison with existing methods for Stokes's integral. manuscripta geodaetica 18(5):227-241.

Heiskanen W H & Moritz H 1967 Physical Geodesy. WH Freeman & Co, San Francisco.

Johnston G M & Featherstone W E 1998 AUSGEOID98 computation and validation: Exposing the hidden dimension. Proceedings of the 39th Australian Surveyors Congress, Launceston, 105-116.

Kirby J F & Featherstone W E 1999 Terrain correcting the Australian gravity data base using the national digital elevation model and the fast Fourier transform. Australian Journal of Earth Sciences 46:555-562.

Kirby J F & Forsberg R 1998 A comparison of techniques for the integration of satellite altimeter and surface gravity data for geoid determination. In: Geodesy on the Move: Gravity, Geoids, Geodynamics, and Antarctica (eds R Forsberg, M Feissl & R Dietrich). Springer, Berlin, 207-212.

Kirby J F, Featherstone W E & Kearsley A H W 1998 Tests of the DMA/GSFC geopotential models over Australia. International Geoid Service Bulletin 7:1-14.

Lemoine FG, Kenyon SC, Factor JK, Trimmer RG, Pavlis NK, Chinn DS, Cox CM, Klosko SM, Luthcke SB, Torrence MH, Wang YM, Williamson RG, Pavlis EC, Rapp RH & Olson TR 1998 The development of the joint NASA GSFC and the National Imagery and Mapping Agency (NIMA) geopotential model EGM96, NASA/TP-1998-206861. National Aeronautics and Space Administration, Maryland, USA.

Martinec Z & Vaníček P 1996 Formulation of the boundary-value problem for geoid determination with a higher-degree reference field. Geophysical Journal International 126:219-228.

Martinec Z, Vaníček P, Mainville A & Véronneau M 1996 Evaluation of topographical effects in precise geoid computation from densely sampled heights. Journal of Geodesy 70:746-754.

Meissl P 1971 Preparations for the numerical evaluation of second-order Molodensky-type formulas. OSU Report 163. Department of Geodetic Science and Surveying, Ohio State University, Columbus, USA.

Molodensky MS, Eremeev VF & Yurkina MI 1962 Methods for Study of the External Gravitational Field and Figure of the Earth. Israeli Programme for the Translation of Scientific Publications, Jerusalem, Israel.

Morgan P, Bock Y, Coleman R, Feng P, Garrard D, Johnston G, Luton G, McDowall B, Pearse M, Rizos C & Tiesler R 1996 A zero-order GPS network for the Australian region. Report ISE-TR 96/60, University of Canberra, Canberra, Australia.

Moritz H 1968 On the use of the terrain correction in solving Molodensky's problem. Report 108. Department of Geodetic Science and Surveying, Ohio State University, Columbus, USA.

Moritz H 1980a Advanced Physical Geodesy. Wichmann, Karlsruhe.

Moritz H 1980b Geodetic Reference System 1980. Bulletin Géodésique 54:395-405.

Paul M K 1973 A method of evaluating the truncation error coefficients for geoidal height. Bulletin Géodésique 47:413-425.

Roelse A, Granger H & Graham J W 1971 The adjustment of the Australian levelling survey - 1970-71. Report 12. National Mapping Council of Australia, Canberra.

Sandwell D T & Smith W H F 1997 Marine gravity anomaly from Geosat and ERS 1 satellite altimetry. Journal of Geophysical Research 102(B5):10039-10054

Schwarz K P, Sideris M G & Forsberg R 1990 The use of FFT techniques in physical geodesy. Geophysical Journal International 100:485-514.

Sideris M G & She B B 1995 A new, high-resolution geoid for Canada and part of the US by the 1D-FFT method. Bulletin Géodésique 69:92-108.

Sjöberg L E 1991 Refined least squares modification of Stokes's formula. manuscripta geodaetica 16:367-375.

Smith D A & Milbert D G 1999 The GEOID96 high-resolution geoid height model for the United States. Journal of Geodesy 73:219-236.

Smith W H F & Wessel P 1990 Gridding with continuous curvature splines in tension. Geophysics 55:293-305.

Stewart M P, Ding X, Tsakiri M & Featherstone W E 1997 The 1996 STATEFIX Project Final Report. Contract Report. School of Surveying and Land Information, Curtin University of Technology, Perth.

Stokes G G 1849 On the variation of gravity on the surface of the Earth. Transactions of the Cambridge Philosophical Society 8:672-695.

Strang van Hees G L 1990 Stokes's formula using fast Fourier techniques. manuscripta geodaetica 15:235-239.

Torge W 1991 Geodesy. de Gruyter, Berlin.

Vaníček P & Featherstone W E 1998 Performance of three types of Stokes's kernel in the combined solution for the geoid. Journal of Geodesy 72:684-697.

Vaníček P & Kleusberg A 1987 The Canadian geoid - Stokesian approach. manuscripta geodaetica 12:86-98.

Vaníček P & Sjöberg L E 1991 Reformulation of Stokes's theory for higher than second-degree reference field and modification of integration kernels. Journal of Geophysical Research 96(B4):6529-6539.

Vincent S & Marsh J G 1973 Global detailed gravimetric geoid. In: Proceedings of the International Symposium on the Use of Artificial Earth Satellites for Geodesy and Geodynamics (ed G Vies). Athens, Greece, 825-855.

Wenzel H-G 1982 Geoid computation by least squares spectral combination using integral kernels, Proceedings of the International Association of Geodesy General Meeting. Tokyo, Japan, 438-453.

Wessel P & Smith W H F 1995 New version of the Generic Mapping Tools released. EOS - Transactions of the American Geophysical Union 76:329.

Wichiencharoen C 1981 The indirect effects on the computation of geoid undulations. Report 336. Department of Geodetic Science and Surveying, Ohio State University, Columbus, USA.

Wong L & Gore R 1969 Accuracy of geoid heights from modified Stokes kernels. Geophysical Journal of the Royal Astronomical Society 18:81-91.

Zhang K F 1997 A comparison of FFT geoid computation techniques and their application to GPS heighting in Australia. PhD Thesis, School of Spatial Sciences, Curtin University of Technology, Perth.